Elliptically polarized modes for the unidirectional excitation of surface plasmon polaritons

Compaijen, Paul J.; Malyshev, Victor A.; Knoester, Jasper

Published in:
Optics Express

DOI:
10.1364/OE.24.003858

Publication date:
2016

Elliptically polarized modes for the unidirectional excitation of surface plasmon polaritons

Paul J. Compaijen, Victor A. Malyshev, and Jasper Knoester*

Zernike Institute for Advanced Materials, University of Groningen, Nijenborgh 4, 9747 AG Groningen, The Netherlands

*j.knoester@rug.nl

Abstract: We propose a new method for the directional excitation of surface plasmon polaritons by a metal nanoparticle antenna, based on the elliptical polarization of the normal modes of the antenna when it is in close proximity to a metallic substrate. The proposed theoretical model allows for the full characterization of the modes, giving the dipole configuration, frequency and lifetime. As a proof of principle, we have performed calculations for a dimer antenna and we report that surface plasmon polaritons can be excited in a given direction with an intensity of more than two orders of magnitude larger than in the opposite direction. Furthermore, using the fact that the response to any excitation can be written as a superposition of the normal modes, we show that this directionality can easily be accessed by exciting the system with a local source or a plane wave. Lastly, exploiting the interference between the normal modes, the directionality can be switched for a specific excitation. We envision the proposed mechanism to be a very useful tool for the design of antennas in layered media.

OCIS codes: (250.5403) Plasmonics; (240.6680) Surface Plasmons; (240.5420) Polaritons; (260.2030) Dispersion.

References

1. W. Barnes, A. Dereux, and T. Ebbesen, "Surface plasmon subwavelength optics," Nature **424**, 824 (2003).
2. E. Ozbay, "Plasmonics: merging photonics and electronics at nanoscale dimensions," Science **311**, 189 (2006).
3. J. A. Schuller, E. S. Barnard, W. Cai, Y. C. Jun, J. S. White, and M. L. Brongersma, "Plasmonics for extreme light concentration and manipulation," Nat. Mater. **9**, 193 (2010).
4. D. K. Gramotnev and S. I. Bozhevolnyi, "Plasmonics beyond the diffraction limit," Nat. Photonics **4**, 83 (2010).
5. N. J. Halas, S. Lal, W.-S. Chang, S. Link, and P. Nordlander, "Plasmons in strongly coupled metallic nanostructures," Chem. Rev. **111**, 3913 (2011).
6. R. Zia, J. A. Schuller, A. Chandran, and M. L. Brongersma, "Plasmonics: the next chip-scale technology," Mater. Today **9**, 20 (2006).
7. D. E. Chang, A. S. Sorensen, P. R. Hemmer, and M. D. Lukin, "Strong coupling of single emitters to surface plasmons," Phys. Rev. B **76**, 035420 (2007).
8. R. F. Oulton, V. J. Sorger, D. A. Genov, D. F. P. Pile, and X. Zhang, "A hybrid plasmonic waveguide for subwavelength confinement and long-range propagation," Nat. Photonics **2**, 496 (2008).
9. A. F. Koenderink, "Plasmon nanoparticle array waveguides for single photon and single plasmon sources," Nano Lett. **9**, 4228 (2009).
10. A. L. Falk, F. H. L. Koppens, C. L. Yu, K. Kang, N. de Leon Snapp, A. V. Akimov, M.-H. Jo, M. D. Lukin, and H. Park, "Near-field electrical detection of optical plasmons and single-plasmon sources," Nat. Phys. **5**, 475 (2009).
11. N. Hartmann, G. Piredda, J. Berthelot, G. Colas Des Francs, A. Bouhelier, and A. Hartschuh, "Launching propagating surface plasmon polaritons by a single carbon nanotube dipolar emitter," Nano Lett. **12**, 177 (2012).

#255340 Received 8 Dec 2015; revised 20 Jan 2016; accepted 21 Jan 2016; published 16 Feb 2016

12. M. S. Tame, K. R. McEnery, . K. Özdemir, J. Lee, S. A. Maier, and M. S. Kim, "Quantum plasmonics," Nat. Phys. **9**, 329 (2013).
13. E. Prodan, C. Radloff, N. J. Halas, and P. Nordlander, "A hybridization model for the plasmon response of complex nanostructures," Science **302**, 419 (2003).
14. P. Nordlander and E. Prodan, "Plasmon hybridization in nanoparticles near metallic surfaces," Nano Lett. **4**, 2209 (2004).
15. G. Lévêque and O. J. F. Martin, "Optical interactions in a plasmonic particle coupled to a metallic film," Opt. Express **14**, 9971 (2006).
16. M. W. Knight, Y. Wu, J. B. Lassiter, P. Nordlander, and N. J. Halas, "Substrates matter: influence of an adjacent dielectric on an individual plasmonic nanoparticle," Nano Lett. **9**, 2188 (2009).
17. F. J. Rodríguez-Fortuño, G. Marino, P. Ginzburg, D. O'Connor, A. Martínez, G. A. Wurtz, and A. V. Zayats, "Near-field interference for the unidirectional excitation of electromagnetic guided modes," Science **340**, 328 (2013).
18. J. P. B. Mueller and F. Capasso, "Asymmetric surface plasmon polariton emission by a dipole emitter near a metal surface," Phys. Rev. B **88**, 121410 (2013).
19. C. Lemke, T. Leissner, A. Evlyukhin, J. W. Radke, A. Klick, J. Fiutowski, J. Kjelstrup-Hansen, H.-G. Rubahn, B. N. Chichkov, C. Reinhardt, and M. Bauer, "The interplay between localized and propagating plasmonic excitations tracked in space and time," Nano Lett. **14**, 2431 (2014).
20. A. B. Evlyukhin and S. I. Bozhevolnyi, "Surface plasmon polariton guiding by chains of nanoparticles," Laser Phys. Lett. **3**, 396 (2006).
21. K. B. Crozier, E. Togan, E. Simsek, and T. Yang, "Experimental measurement of the dispersion relations of the surface plasmon modes of metal nanoparticle chains," Opt. Express **15**, 17482 (2007).
22. D. Brunazzo, E. Descrovi, and O. J. F. Martin, "Narrowband optical interactions in a plasmonic nanoparticle chain coupled to a metallic film," Opt. Lett. **34**, 1405 (2009).
23. A. Farhang, S. A. Ramakrishna, and O. J. F. Martin, "Compound resonance-induced coupling effects in composite plasmonic metamaterials," Opt. Express **20**, 29447 (2012).
24. P. J. Compaijen, V. A. Malyshev, and J. Knoester, "Surface-mediated light transmission in metal nanoparticle chains," Phys. Rev. B **87**, 205437 (2013).
25. P. J. Compaijen, V. A. Malyshev, and J. Knoester, "Engineering plasmon dispersion relations: hybrid nanoparticle chain-substrate plasmon polaritons," Opt. Express **23**, 2280 (2015).
26. F. Bernal Arango, A. Kwadrin, and A. F. Koenderink, "Plasmonic antennas hybridized with dielectric waveguides," ACS Nano **6**, 10156 (2012).
27. R. de Waele, A. F. Koenderink, and A. Polman, "Tunable nanoscale localization of energy on plasmon particle arrays," Nano Lett. **7**, 2004 (2007).
28. A. V. Malyshev, V. A. Malyshev, and J. Knoester, "Frequency-controlled localization of optical signals in graded plasmonic chains," Nano Lett. **8**, 2369 (2008).
29. P. Bharadwaj, B. Deutsch, and L. Novotny, "Optical antennas," Adv. Opt. Photonics **1**, 438 (2009).
30. L. Novotny and N. van Hulst, "Antennas for light," Nat. Photonics **5**, 83 (2011).
31. T. Coenen, E. J. R. Vesseur, A. Polman, and A. F. Koenderink, "Directional emission from plasmonic Yagi-Uda antennas probed by angle-resolved cathodoluminescence spectroscopy," Nano Lett. **11**, 3779 (2011).
32. R. S. Pavlov, A. G. Curto, and N. F. van Hulst, "Log-periodic optical antennas with broadband directivity," Opt. Commun. **285**, 3334 (2012).
33. J. Munárriz, A. V. Malyshev, V. A. Malyshev, and J. Knoester, "Optical nanoantennas with tunable radiation patterns," Nano Lett. **13**, 444 (2013).
34. J. Lin, J. P. B. Mueller, Q. Wang, G. Yuan, N. Antoniou, X.-C. Yuan, and F. Capasso, "Polarization-controlled tunable directional coupling of surface plasmon polaritons," Science **340**, 331 (2013).
35. A. Pors, M. G. Nielsen, T. Bernardin, J.-C. Weeber, and S. I. Bozhevolnyi, "Efficient unidirectional polarization-controlled excitation of surface plasmon polaritons," Light: Sci. Appl. **3**, e197 (2014).
36. J. Yang, X. Xiao, C. Hu, W. Zhang, S. Zhou, and J. Zhang, "Broadband surface plasmon polariton directional coupling via asymmetric optical slot nanoantenna pair," Nano Lett. **14**, 704 (2014).
37. D. Zhu, Z. Dong, H.-S. Chu, Y. A. Akimov, and J. K. W. Yang, "Image dipole method for the beaming of plasmons from point sources," ACS Photonics **1**, 1307 (2014).
38. Z. Dong, H.-S. Chu, D. Zhu, W. Du, Y. A. Akimov, W. P. Goh, T. Wang, K. E. J. Goh, C. Troadec, C. A. Nijhuis, and J. K. W. Yang, "Electrically-excited surface plasmon polaritons with directionality control," ACS Photonics **2**, 385 (2015).
39. W. Yao, S. Liu, H. Liao, Z. Li, C. Sun, J. Chen, and Q. Gong, "Efficient directional excitation of surface plasmons by a single-element nanoantenna," Nano Lett. **15**, 3115 (2015).
40. M. Neugebauer, T. Bauer, P. Banzer, and G. Leuchs, "Polarization tailored light driven directional optical nanobeacon," Nano Lett. **14**, 2546 (2014)
41. S.-Y. Lee, I.-M. Lee, J. Park, S. Oh, W. Lee, K.-Y. Kim, and B. Lee, "Role of magnetic currents in nanoslit excitation of surface plasmon polaritons," Phys. Rev. Lett. **108**, 213907 (2012).
42. Y. O. Nakamura, "Spin quantum number of surface plasmon," Solid State Commun. **39**, 763 (1981)

#255340 Received 8 Dec 2015; revised 20 Jan 2016; accepted 21 Jan 2016; published 16 Feb 2016

43. K. Y. Bliokh and F. Nori, "Transverse spin of a surface polariton," Phys. Rev. A **85**, 061801 (2012)
44. S.-Y. Lee, I.-M. Lee, K.-Y. Kim, and B. Lee, "Comments on "Near-field interference for the unidirectional excitation of electromagnetic guided modes"," arXiv:1306.5068v1 (2013)
45. F. J. Rodríguez-Fortuño, G. Marino, P. Ginzburg, D. O'Connor, A. Martnez, G. A. Wurtz, and A. V. Zayats, "Regarding the "Comments on 'Near-field interference for the unidirectional excitation of electromagnetic guided modes," by Lee et al," arXiv:1307.0218v2 (2013)
46. B. le Feber, N. Rotenburg, and K. Kuipers, "Nanophotonic control of circular dipole emission," Nat. Commun. **6**, 6695 (2015)
47. R. Mitsch, C. Sayrin, B. Albrecht, P. Schneeweiss, and A. Rauschenbeutel, "Quantum state-controlled directional spontaneous emission of photons into a nanophotonic waveguide," Nat. Commun. **5**, 5713 (2014)
48. J. Petersen, J. Volz, and A. Rauschenbeutel, "Chiral nanophotonic waveguide interface based on spin-orbit interaction of light," Science **346**, 67 (2014).
49. K. Y. Bliokh, D. Smirnova, and F. Nori, "Quantum spin Hall effect of light," Science **348**, 1448 (2015).
50. K. Y. Bliokh, F. J. Rodríguez-Fortuño, F. Nori, and A. V. Zayats, "Spin-orbit interactions of light," Nat. Photonics **9**, 796 (2015)
51. S. Y. Park and D. Stroud, "Surface-plasmon dispersion relations in chains of metallic nanoparticles: an exact quasistatic calculation," Phys. Rev. B **69**, 125418 (2004).
52. M. Meier and A. Wokaun, "Enhanced fields on large metal particles: dynamic depolarization," Opt. Lett. **8**, 581 (1983).
53. V. A. Markel and A. K. Sarychev, "Propagation of surface plasmons in ordered and disordered chains of metal nanospheres," Phys. Rev. B **75**, 085426 (2007).
54. W. H. Weber and G. W. Ford, "Propagation of optical excitations by dipolar interactions in metal nanoparticle chains," Phys. Rev. B **70**, 125429 (2004).
55. A. Alù and N. Engheta, "Theory of linear chains of metamaterial/plasmonic particles as subdiffraction optical nanotransmission lines," Phys. Rev. B **74**, 205436 (2006).
56. S. Campione, S. Steshenko, and F. Capolino, "Complex bound and leaky modes in chains of plasmonic nanospheres," Opt. Express **19**, 18345 (2011).
57. A. F. Koenderink and A. Polman, "Complex response and polariton-like dispersion splitting in periodic metal nanoparticle chains," Phys. Rev. B **74**, 033402 (2006).
58. L. Novotny and B. Hecht, *Principles of Nano-optics* (Cambridge University, 2006).
59. W. C. Chew, *Waves and Fields in Inhomogeneous Media* (IEEE, 1999).
60. M. Paulus, P. Gay-Balmaz, and O. Martin, "Accurate and efficient computation of the Green's tensor for stratified media," Phys. Rev. E **62**, 5797 (2000).
61. A. F. Koenderink, R. de Waele, J. C. Prangsma, and A. Polman, "Experimental evidence for large dynamic effects on the plasmon dispersion of subwavelength metal nanoparticle waveguides," Phys. Rev. B **76**, 201403 (2007).
62. V. A. Markel, "Antisymmetrical optical states," J. Opt. Soc. Am. B **12**, 1783 (1995).
63. T. Brixner and G. Gerber, "Femtosecond polarization pulse shaping," Opt. Lett. **26**, 557 (2001).
64. M. Aeschlimann, M. Bauer, D. Bayer, T. Brixner, F. J. G. De Abajo, W. Pfeiffer, M. Rohmer, C. Spindler, and F. Steeb, "Adaptive sub-wavelength control of nanoscopic fields," Nature **446**, 301 (2007).
65. A. L. Koh, A. I. Fernández-Domínguez, D. W. McComb, S. A. Maier, and J. K. W. Yang, "High-resolution mapping of electron-beam-excited plasmon modes in lithographically defined gold nanostructures," Nano Lett. **11**, 1323 (2011).
66. T. Coenen, F. Bernal Arango, A. F. Koenderink, and A. Polman, "Directional emission from a single plasmonic scatterer," Nat. Commun. **5**, 3250 (2014).

1. Introduction

Plasmons hold great promise for the field of nanophotonics, since these electromagnetic waves can be confined well below the diffraction limit and can propagate over distances of several tens of microns [1–5]. These properties make plasmonic structures the ideal platform for studying single emitters, as well as for designing nanophotonic circuitry [6–12].

Of particular importance are Surface Plasmon Polaritons (SPPs), propagating surface waves which can be excited on the interface between a dielectric and a metal. Since these are guided modes, they cannot be excited by direct illumination, but some phase-matching techniques are needed. A common approach is to use a local emitter, for example the plasmon resonance of a metal nanoparticle (MNP), as a near-field source for the excitation of the guided modes. The presence of the substrate will also affect the optical response of the MNP, the plasmon of the MNP will mix with the modes of the substrate. A very clear description of this phenomena can be given in the framework of plasmon hybridization [13, 14]. For a single MNP close to a

#255340 Received 8 Dec 2015; revised 20 Jan 2016; accepted 21 Jan 2016; published 16 Feb 2016

substrate, resonance frequency shifts and high field intensities in the gap have been observed, as well as the interplay between the localized plasmon of the MNP and the propagating SPP [15–19]. When a chain of MNPs close to a metallic substrate is considered, the hybrid modes of the system are shown to have interesting properties, such as guiding, bending and negative phase velocity [20–25].

For applications in nano-photonic circuitry and sensing, it is desired to be able to excite guided modes with a preferred direction. An important step towards achieving this goal was taken by hybridizing a plasmonic antenna with a dielectric waveguide. The antenna couples the free-space radiation directionally to the confined modes of the waveguide and vice versa [26]. Plasmonic antennas can be created from collections of metal nanoparticles (MNPs) and can be designed to have specific properties, like localization and directivity [9, 27–33]. Most commonly used are the so-called phased array antennas, in which the directionality is obtained by engineering the constructive and destructive interference between the antenna elements. Based on this approach, antennas have been created that allow for polarization-dependent, directional excitation of SPPs [34, 35]. Alternatively, grooves in a metallic substrate have been used as antenna elements and directionality is obtained due to the interference of the electric field scattered from separate grooves [36–38], or even due to the interference of the modes of a single, structured groove [39].

In [17, 18, 40], it was reported that directional excitation of guided modes can even be obtained from a single metal nanoparticle, provided its induced dipole moment is out-of-plane circularly polarized. In particular, these references have studied the directional excitation of SPPs by circularly polarized MNP above a metal substrate. The phase difference between the dipole moment parallel and perpendicular to the waveguide gives rise to constructive interference in one direction, and destructive inference in the opposing direction. Optimizing the system can even lead to a complete cancellation of SPPs in a particular direction [18]. The first experimental realization of the directional excitation of SPPs by using circularly polarized light was achieved using a nanoslit rather than a metal nanoparticle [41]. Later, the effect was demonstrated for a single optical nano-antenna by exciting it with a polarization tailored beam [40]. Directional emission from circularly polarized dipoles can also be explained in the context of angular momentum matching. For surface polaritons, spin and propagation direction are coupled, and therefore a circularly polarized dipole will preferentially excite SPPs with one particular propagation direction [42, 43]. Over the last few years, there has been a great effort in getting a better fundamental understanding of the important physics, see e.g. the discussion in [44, 45], and finding new implementations of this phenomenon [46–49]. A clear overview of recent progress is given in [50].

In order to achieve a circularly, or in general elliptically, polarized dipole, the external excitation needs to be elliptically polarized. In practice, this will limit the applicability of this method and, furthermore, it can be complicated to excite the system with a specific elliptically polarized beam when the system is embedded in a layered structure. In this paper, we will demonstrate a new mechanism for obtaining directional near-field excitation of SPPs, based on the elliptical polarization of the plasmonic modes of coupled MNPs above a metallic substrate. The method for finding the collective modes of the hybrid system is presented and, as a proof of principle, we will discuss the results for an asymmetric dimer above a metallic substrate and show that it contains normal modes which couple directionally to SPPs. Since this effect originates from the modes of the system, the directionality is inherent, i.e. it does not rely on elliptically polarized excitation.

#255340 Received 8 Dec 2015; revised 20 Jan 2016; accepted 21 Jan 2016; published 16 Feb 2016

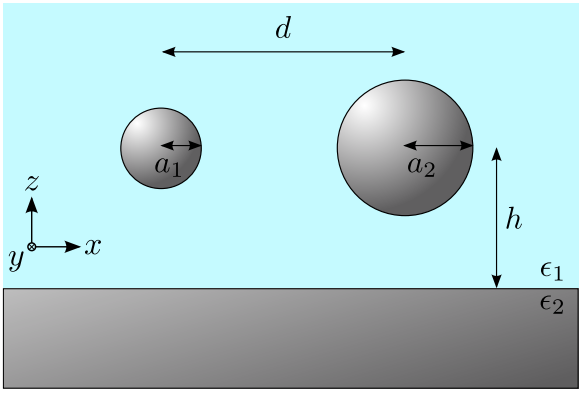

Fig. 1. A schematic illustration of the considered system: a dimer of silver nanospheres with different sizes, embedded in medium 1, located above and parallel to a metallic substrate (medium 2). a_1 and a_2 are the radii of particle 1 and 2, respectively, d is the center-to-center spacing between the MNPs and h is the distance from the dimer to the substrate. Throughout this work, we will consider the metallic substrate to be silver and the embedding medium to be glass.

2. Formalism

The calculations presented in this paper are based on a coupled dipoles approach, i.e., the MNPs are treated as point dipole scatterers and the coupling between the MNPs is taken into account using dipole-dipole interactions, including retardation effects. The interaction with the substrate is calculated from the recipe prescribed by Sommerfeld. For a dimer of MNPs, which is the system of interest, the geometry of the system under consideration is shown in Fig. 1. The radii of the particles are given by a_1 and a_2 respectively, the center-to-center spacing between the particles is given by d, and the dimer is situated at a height h from the substrate. The formalism presented below may easily be generalized to arrays of an arbitrary number of MNPs placed parallel to the substrate. We stress that all calculations have been performed under conditions for which the point dipole approximation is known to be valid [24, 51], i.e. the particle radii are much smaller than the wavelength, and the spacing and height satisfy $d \geq 3a$ and $h \geq 2a$. Therefore, the dipole model provides an excellent framework to perform the calculations, without obscuring the important physical phenomena that are necessary for a deep understanding.

In order to understand the collective resonances of the hybrid system, it is useful to first consider only a single isolated spherical MNP. Assuming the particle is much smaller than the wavelength, the dipole moment induced in the MNP will be $\mathbf{p} = \varepsilon_1 \alpha \mathbf{E}$, where ε_1 is the permittivity of the dielectric (medium 1), $\mathbf{E}$ is the electric field exciting the particle, and $\alpha(\omega)$ is the frequency dependent polarizability of the MNP, given by

$$\frac{1}{\alpha(\omega)} = \frac{\varepsilon_{MNP}(\omega) + 2\varepsilon_1}{\varepsilon_{MNP}(\omega) + \varepsilon_1} \frac{1}{a^3} - \frac{k_1^2}{a} - \frac{2i}{3} k_1^3. \tag{1}$$

The first term of this equation is the polarizability as derived from electrostatics, with ε_{MNP} representing the permittivity of the MNP. The second and third terms are dynamical corrections taking into account spatial dispersion and radiation damping [52, 53]. The wavevector in the surrounding medium is defined as $k_1 = \sqrt{\varepsilon_1}\omega/c$. Generally, since the MNP is a metallic particle, it has a Drude-type permittivity and it is important to take into account the ohmic losses. Calculating $|\alpha|^2$ from Eq. (1) as a function of ω shows a Lorentzian-like response with a strong peak and well-defined width. The peak is the plasmon resonance frequency of the metal

#255340 Received 8 Dec 2015; revised 20 Jan 2016; accepted 21 Jan 2016; published 16 Feb 2016

nanoparticle and the width is due to both the ohmic and the radiation losses. The resonance in fact corresponds to exciting the normal mode of the MNP, which has a corresponding complex normal mode frequency. The real part of this frequency corresponds to the peak position, while the imaginary part is associated with the Full Width Half Maximum of the peak. The normal mode frequency corresponds to the singularity of the polarizability, i.e., the frequency for which the dipole moment of the MNP becomes infinite.

In a dimer, each MNP does not only experience the monochromatic external field $\mathbf{E}^{\text{ext}}$, but also the field generated by the other particle. Within the Green's tensor formalism, the electric field at position $\mathbf{r}$ generated by a point dipole $\mathbf{p}'$ located at $\mathbf{r}'$ and oscillating with frequency ω is given by

$$\mathbf{E}(\mathbf{r}) = \frac{k_1^2}{\varepsilon_1}\hat{\mathbf{G}}(\omega, \mathbf{r}, \mathbf{r}')\mathbf{p}', \tag{2}$$

where $\hat{\mathbf{G}}(\omega, \mathbf{r}, \mathbf{r}')$ is the 3 by 3 electromagnetic Greens tensor. Hence, for a dimer the dipoles of the MNPs are governed by the following system of coupled equations

$$\frac{1}{\varepsilon_1}\begin{pmatrix} \frac{1}{\alpha_1(\omega)}\hat{\mathbf{I}} & -k_1^2\hat{\mathbf{G}}(\omega, \mathbf{r_1}, \mathbf{r_2}) \\ -k_1^2\hat{\mathbf{G}}(\omega, \mathbf{r_2}, \mathbf{r_1}) & \frac{1}{\alpha_2(\omega)}\hat{\mathbf{I}} \end{pmatrix}\begin{pmatrix} \mathbf{p_1} \\ \mathbf{p_2} \end{pmatrix} = \begin{pmatrix} \mathbf{E_1^{\text{ext}}} \\ \mathbf{E_2^{\text{ext}}}, \end{pmatrix} \tag{3}$$

or, in short, $\hat{\mathbf{M}}\mathbf{p} = \mathbf{E}$, where $\hat{\mathbf{M}}$ is a 6x6 matrix, and $\mathbf{p}$ and $\mathbf{E}$ are 1x6 vectors. For the general case of N particles the system will be of dimensions $3N$x$3N$. This equation allows one to calculate the dipole moments induced in the MNPs given a specific excitation, or reversely, the electric field produced for a given set of dipoles. Mathematically, this system is very similar to a set of driven coupled harmonic oscillators. Physically, one gains a great deal of insight into these systems by calculating the so-called quasinormal modes, and their corresponding complex frequencies. In this work, we will refer to these modes simply as normal modes, however all losses are properly taken into account. The real part of the frequency corresponds to the oscillation frequency of the dipoles and the imaginary part is the inverse lifetime of the mode. To find the normal modes of such a system, the homogeneous equation has to be solved, by setting $\mathbf{E} = 0$. This implies that the complex frequencies corresponding to $\det(\hat{\mathbf{M}}) = 0$ have to be found and subsequently the eigenvalue problem has to be solved for each of those frequencies. This procedure is carefully described in, for example [53–56]. In this study, the positions of the roots of the determinant were first estimated by calculating $|\det(\hat{\mathbf{M}})|$ on the complex frequency plane, which were then used as an input for the build-in rootfinder of Matlab R2015a.

Since losses are inherent to the system, the normal modes will in general not be orthogonal. However, they do form a complete set and therefore it is still possible to expand any solution of $\mathbf{p}$ as a superposition of the normal modes. This can be achieved by constructing a so-called bi-orthogonal system (see Appendix A).

It is important to note that calculating the normal modes for a given system becomes numerically more difficult for increasing system size. The reason lies in the calculation of the interaction at complex frequency which diverges at large distances, because the electric field at large distances diverges. Assuming a time-dependence of $\exp[-i\omega t]$, implies that the normal mode frequencies have to satisfy $\text{Im}[\omega] < 0$ in order to obtain modes that are decaying in time. Inserting such a frequency in a propagating wave $\exp[ikr] = \exp[i\omega r/c]$ gives a wave that is growing as it propagates. It is important to realize that this does not violate causality, in reality there is a wavefront $r/c = t$ at which the decay in time and the increase in distance exactly cancel and no interactions can occur before the wavefront arrives. For infinitely long chain of MNPs this difficulty can be circumvented by assuming Bloch modes and using analytical continuation to calculate the dipole sums forming the interaction [57].

#255340 Received 8 Dec 2015; revised 20 Jan 2016; accepted 21 Jan 2016; published 16 Feb 2016

Needless to say, the normal modes will be determined to a large extent by the detailed form of $\hat{\mathbf{G}}$, which in turn depends strongly on the environment. For a dipole in a homogeneous medium, the tensor is often referred to as $\hat{\mathbf{G}}^H$ and is defined in Cartesian coordinates as [58]

$$\hat{\mathbf{G}}^H(\omega;\mathbf{r},\mathbf{r}') = \left[\hat{\mathbf{I}} + \frac{\nabla\nabla}{k_1^2}\right]\frac{\exp(ik_1|\mathbf{r}-\mathbf{r}'|)}{|\mathbf{r}-\mathbf{r}'|}\ . \tag{4}$$

From the above equation it is obvious that if $\mathbf{r}-\mathbf{r}'$ is parallel to one of the coordinate axes, the tensor will be diagonal, i.e. $G_{ij} = 0$ if $i \neq j$, hence the three different polarizations are completely decoupled. For a linear chain of dipoles in a homogeneous medium this will always be the case and therefore the modes of such a chain will always be linearly polarized.

In general, any inhomogeneity that is introduced into the system will break its symmetry and therefore gives rise to a cross-coupling between the different polarizations. In particular, for the set-up considered in this paper (see Fig. 1), the presence of the substrate introduces a coupling between x and z-polarized modes. In this case, there are two possible interaction paths between the particles, a direct one, mediated by free-space photons, and an indirect path, comprising contributions both from reflections and SPPs at the substrate. In general, the two interactions will have a different polarization and phase, resulting in an elliptically polarized field at the particle position, and hence, in elliptically polarized dipoles, with a polarization oscillating in the xz-plane.

To characterize the phase difference and the resulting polarization, one needs to calculate the Green's tensor for an oscillating dipole located above a metallic substrate. A well-known approach for this was developed by Sommerfeld, and is based on expanding the dipole field into a product of cylindrical waves and plane waves for which the interaction with the substrate is simply given by Fresnel reflection [58–60]. In particular, the Fresnel coefficient for TM polarized light will describe the coupling to the SPP of the substrate. The outlined procedure results in contour integrals that have to be calculated numerically. Extra care needs to be taken when calculating the normal modes for this system, since the integrals then have to be evaluated for complex frequency, so that the convergence is very sensitive to the choice of the integration path and the branch cuts. This is explained in more detail in Appendix B.

3. Results and discussion

To illustrate the above we have performed calculations for a dimer of silver nanospheres above a silver substrate (see Fig. 1). To describe the frequency dependent permittivity of silver a generalized Drude model is used [61],

$$\varepsilon_{MNP} = \varepsilon_2 = \varepsilon(\omega) = 5.45 - 0.73\ \frac{\omega_p^2}{(\omega^2 + i\omega\gamma)}, \tag{5}$$

with plasma frequency $\omega_p = 17.2$ rad fs^{-1} and damping coefficient $\gamma = 0.0835$ fs^{-1}. The surrounding medium is chosen to be glass with $\varepsilon_1 = 2.25$.

In order to make this paper reasonably self-contained, we will first briefly discuss the optical response of a single silver MNP above a silver substrate. In Fig. 2(a), the dispersion relation of the SPP on the silver substrate is given. The surface plasmon frequency, ω_{sp}, and the resonance frequency of the MNP, ω_{MNP}, are indicated by the dotted lines. It is important to note that the SPP results from hybridization of the surface plasmon of the metal and the photons in the dielectric. From the SPP dispersion relation it can be seen that the MNP plasmon resonance has an appropriate frequency to couple to the SPPs of the substrate. Figure 2(b) gives the optical response, i.e. the modulus squared of the dipole moment of a silver MNP situated at $h = 50$ nm above the substrate. The particle is excited by a stationary z-polarized electric field with angular

#255340 Received 8 Dec 2015; revised 20 Jan 2016; accepted 21 Jan 2016; published 16 Feb 2016

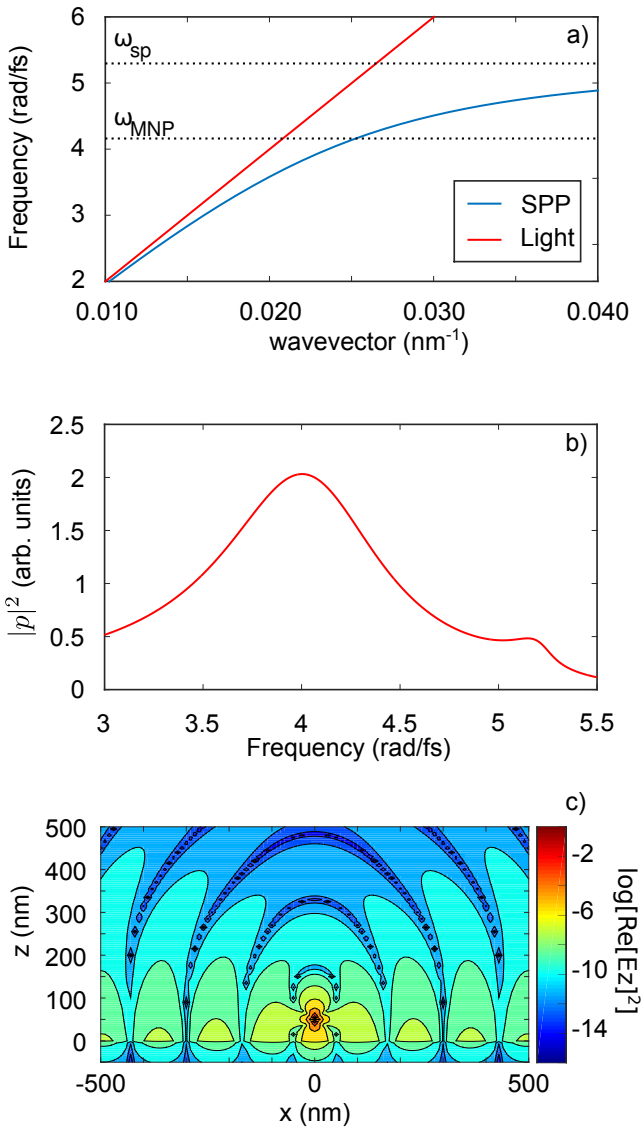

Fig. 2. (a) SPP dispersion on the interface between silver and glass. Also indicated are: (i) the resonance frequency ω_{MNP} of a silver MNP with a radius of $a = 25$ nm, (ii) the frequency of the surface plasmon resonance ω_{sp}, (iii) the lightline in glass. (b) The modulus squared of the dipole moment of a silver MNP located in glass at $h = 50$ nm above the glass-silver interface, induced by a stationary z-polarized electric field of angular frequency ω. (c) Logarithmic plot of the square of the real part of the z-component of the electric field that is produced by the MNP is plotted in the xz-plane ($y = 0$) for an excitation frequency of $\omega = 4$ rad/fs (highest peak in panel (b)). The system's geometry is the same as in panel (b).

frequency ω. In this graph, two peaks can be distinguished: one close to the MNP resonance, the other close to the surface plasmon of the substrate. The relatively large frequency spacing between both resonances implies that the hybrid MNP-substrate modes will be closely related to their non-interacting constituents. In Fig. 2(c), the square of the real part of the z-component

#255340 Received 8 Dec 2015; revised 20 Jan 2016; accepted 21 Jan 2016; published 16 Feb 2016

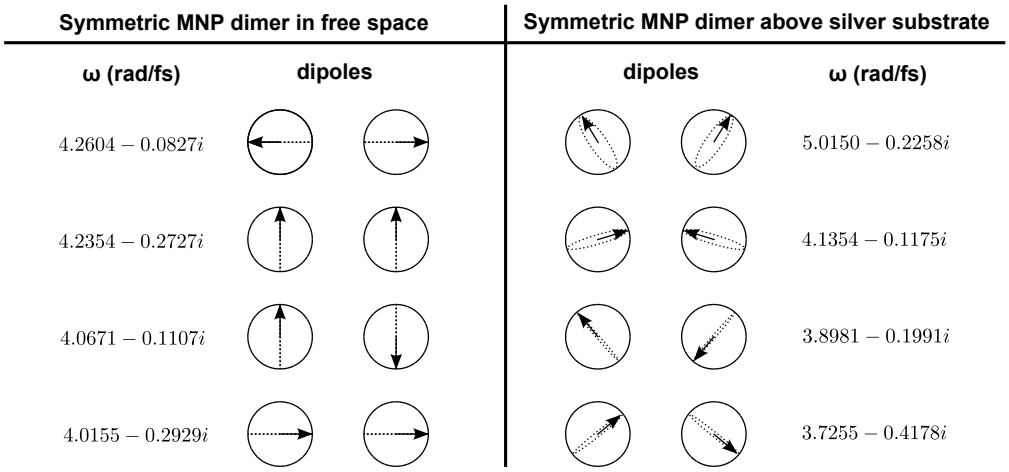

Fig. 3. The modes of a dimer comprising two equal-size silver MNPs embedded in glass are shown, with (right) and without (left) the presence of a silver substrate, using $a = 25$, $d = 90$ and $h = 50$ nm. The black arrow indicates the dipole moment, while the dashed line represents the contour traced out by the dipole as a function of time. For each mode the complex normal mode frequency ω in units of rad/fs is also given.

of the electric field is shown on a logarithmic scale, when the MNP is excited resonantly. The high intensity close to the substrate is a clear indication that indeed SPPs are excited.

We will now turn to the modes of a symmetric MNP dimer above a silver substrate. In Fig. 3 it is shown how the well-known modes of a dimer, consisting of two equal particles, are changed when a silver substrate is present. The modes depicted here were found by solving Eq. (3) for $\mathbf{E} = \mathbf{0}$ under the given conditions. Generally, the presence of the substrate will give rise to three effects: the cross-coupling of longitudinal and transversal modes, shifts of the resonance frequencies due to the interaction with the reflected field, and, to a smaller extent, the hybridization of the dimer modes with the surface plasmon of the substrate. In Fig. 3, the cross-coupling between the longitudinal and transversal modes is obvious from the tilted dipoles. Depending on the phase difference between the two polarizations, the amplitudes of the dipoles trace a straight line (no phase difference) or, in general, an ellipse. Comparing the left and the right panel of Fig. 3 it becomes clear that not only the dipole moments are altered, but also the resonance frequencies have changed. These shifts result from the change in the effective inter-particle coupling due to the field that is reflected from the substrate. There is also a contribution from the hybridization of the dimer modes with the surface plasmon. However, due to the large frequency separation between the isolated dimer and the surface plasmon, the effect is very small. Therefore, we can assume that modes that are depicted here mainly originate from the dimer. It is important to note that the system contains many more normal modes, which occur at higher frequency and mainly correspond to the substrate.

As expected, some of the modes of the MNP dimer above the substrate, shown in Fig. 3, indeed contain elliptically polarized dipoles. According to [17, 18], dipoles with such a polarization can excite SPPs in a preferred direction. However, due to the symmetry of the geometry considered here, both MNPs cause fields of opposite directionality, yielding a net non-directional response. This effect can be easily overcome by lifting the symmetry of the system. To this end, we consider a dimer consisting of two silver nanospheres with different sizes. Other approaches may be using particles of different shape or different material. Figure 4 shows the normal modes and the corresponding frequencies for a dimer consisting of silver nanospheres

#255340 Received 8 Dec 2015; revised 20 Jan 2016; accepted 21 Jan 2016; published 16 Feb 2016

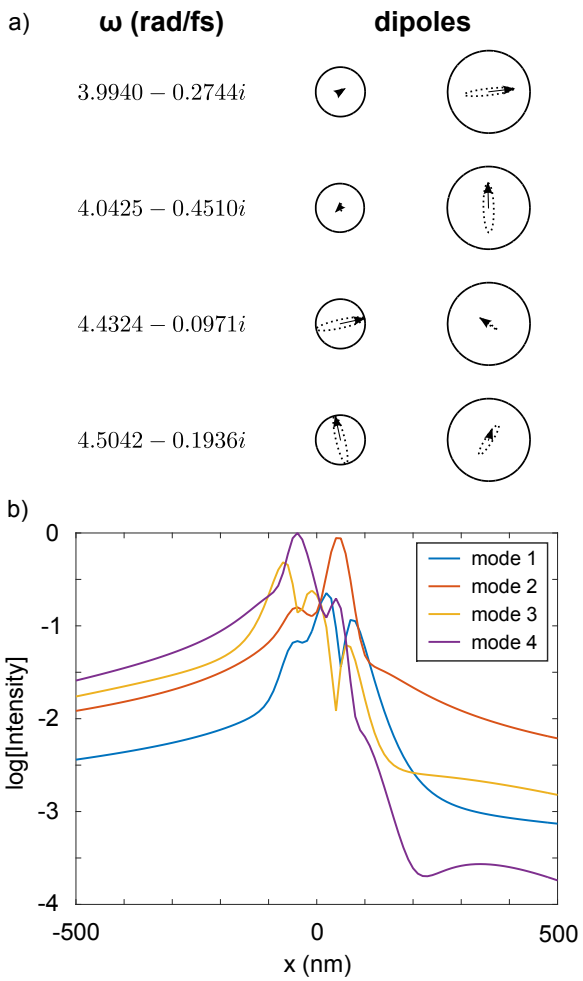

Fig. 4. (a) As in the right panel of Fig. 3, but now for an asymmetric dimer, with particle sizes $a_1 = 15$ and $a_2 = 25$ nm, respectively. The asymmetry and ellipticity of the modes are clearly seen from the arrows representing the dipole moments. (b) The intensity of the electric field generated as a function of x along the line $y = 0, z = 5$ nm by each of the modes depicted in (a). The modes are normalized and the intensity is scaled in such a way that the highest peak in mode 4 equals 1. All modes radiate more in the -x direction and this effect is the strongest for mode 4.

with sizes of $a_1 = 15$ nm and $a_2 = 25$ nm, respectively. As can be seen from this figure, the asymmetry results in modes that are mainly localized on one of the particles and show strong asymmetry with respect to $x = 0$. Therefore, the optical response of the system will be asymmetric and directional excitation of SPPs on the substrate can be achieved.

To illustrate the directional response of this system, Fig. 5 shows the radiation profiles of the asymmetric dimer above a silver substrate. The dipoles of the MNPs are assumed to oscillate according to mode 4 of Fig. 4, i.e., only this mode is considered to be excited. In Fig. 5(a) the square of the real part of the z-component of the electric field is plotted. The bright spots show the position of the dimer and the coupling of the dimer to the SPP for this mode is seen from the high intensity wave that is propagating on the substrate. It is clear from the figure that the

#255340 Received 8 Dec 2015; revised 20 Jan 2016; accepted 21 Jan 2016; published 16 Feb 2016

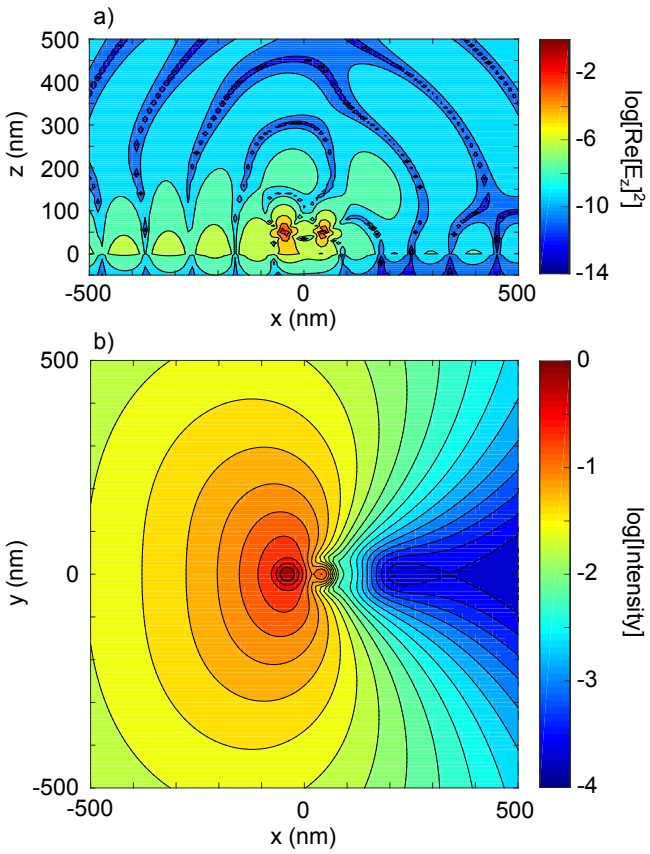

Fig. 5. The radiation profiles of the asymmetric dimer are plotted. In both cases, the field produced by mode 4 of Fig. 4 is shown. (a) The square of the real part of the z-component of the electric field in the xz-plane. (b) The normalized electric field intensity profile on a plane parallel to the xy-plane, at a height of $z = 5$ nm above the substrate. Both pictures show a strong asymmetry along the x-axis, with an intensity contrast of a factor of 140 between $x = +500$ and $x = -500$ nm along the line $y = 0$ nm.

excitation of the SPP by the dimer is strongly asymmetric. This is further illustrated in Fig. 5(b) in which the normalized intensity of the electric field is plotted on a surface that is parallel to and at a height of $z = 5$ nm above the substrate. As can be seen, the strong asymmetry does not only occur close to the dimer axis: over a width of about 100 nm transverse to the dipole axis there is a large intensity contrast visible. The intensity contrast along the x-axis is characterized by a factor of 140 between $x = +500$ and $x = -500$ nm. It should be pointed out that the radiation profile of an asymmetric dimer in free space also is directional, however, much less pronounced. In absence of the substrate, the most directional normal mode has an intensity contrast along the same line of only a factor of 5.

So far we have shown that the considered system has quasi-normal modes which can directionally excite SPPs. It is an inherent property of the system, since those modes exist without any external excitation. Therefore, no external source of elliptically polarized light is needed. However, in order to use this mechanism to directionally excite guided modes, an important question arises: how to supply energy to the modes that are responsible for the directionality? In the present situation, a strong intensity contrast of two orders of magnitude is only seen for

#255340 Received 8 Dec 2015; revised 20 Jan 2016; accepted 21 Jan 2016; published 16 Feb 2016

mode 4 (see Fig. 4(b)) and therefore, it is crucial to be able to couple most of the excitation to this specific mode. As was mentioned earlier, the response of the system to any excitation, can be written in terms of a superposition of the system's normal modes (see Appendix A). The prefactors in the superposition will depend on the frequency and the polarization of the given excitation. Due to the presence of both Ohmic and radiative losses, the spectral dependence of each mode is relatively broad and, because of that, there is a significant overlap between the modes.

Furthermore, the fact that the modes are not orthogonal makes it less straightforward to use polarization to select one particular mode: even if the provided excitation is such that the polarization and phase of the electric field acting at the location of each particle match exactly to one of the modes, still a superposition of multiple modes will be excited. Here "match exactly" means that the electric field at each particle has a direction parallel to the mode's dipole on that particle, while the ratio of the electric field amplitudes and their relative phases at both particles equal the amplitude ratio and phase difference for the mode's dipoles on both particles. However, it is worth noting that there are techniques available to optimize the excitation of one particular mode, even under these conditions. Let us denote the set of non-orthogonal modes $\mathbf{v}_i$, where i denotes the mode index and $\mathbf{v}$ is a complex vector with length 4, corresponding to the x and z polarization of both particles. Then, a corresponding bi-orthogonal set $\mathbf{v}^i$ can be constructed [62], which has the property that $\mathbf{v}^i\mathbf{v}_j = \delta_{i,j}$, where $\delta_{i,j}$ is the Kronecker delta. Exciting the system along one of the vectors $\mathbf{v}^i$ (i.e. choosing the electric field values at both particles such that their orientations, phases, and amplitude ratio matches $\mathbf{v}^i$), implies that the excitation will only couple to mode $\mathbf{v}_i$. Therefore, to excite only a single mode the excitation should not be matched to the mode itself, but to its counterpart in the bi-orthogonal set. In order to achieve such an excitation, beam shaping techniques with which both amplitude and polarization of the input electric field can be altered, might be needed [63, 64]. However, since the directionality is an inherent property of the system, even standard excitations, such as near field excitation or plane wave excitation yield a significant directionality. As is seen from the mode configurations in Fig. 4(a), the modes are mainly localized on one of the particles. This implies that the modes are very sensitive to a local excitation. From Fig. 4(b) one can recognize that mode 4 will couple strongly to a z-polarized CW excitation at the smaller MNP, with a frequency of $\omega = 4.50$ rad/fs. The response of the dimer to this particular excitation (Excitation 1), is plotted as the blue solid line in Fig. 6. Even though a complex superposition of the modes is excited, still a strongly directional response of more than one order of magnitude is observed. In practice, such excitation conditions can be easily achieved by making use of near field excitation with an optical fiber, or electronically with cathodoluminescence [31, 65, 66]. Interestingly, since the modes in a superposition have different phases and amplitudes, interference between the normal modes can occur, which can lead to counterintuitive phenomena. An example is depicted for Excitation 2 in Fig. 6, the response of the system to an equal z-polarized CW electric field at both MNPs with a frequency of $\omega = 4.85$ rad/fs. The response shows a preferred emission in the $+x$ direction, whereas all modes (see Fig. 4(b)) show a directionality in the $-x$ direction. Calculating the radiation of each of the modes separately, revealed that modes 2 and 4 are destructively interfering in the $-x$ direction, whereas there is constructive interference in the $+x$ direction, yielding a net directional response in the $+x$ direction.

4. Summary

We have provided a method which can be used to find the normal modes of a collection of metal nanoparticles above a metallic substrate. The modes of such system are shown to be elliptically polarized. Using the fact that elliptically polarized dipoles can directionally excite surface plasmon polaritons on the metallic substrate, we have designed a system for which

#255340 Received 8 Dec 2015; revised 20 Jan 2016; accepted 21 Jan 2016; published 16 Feb 2016

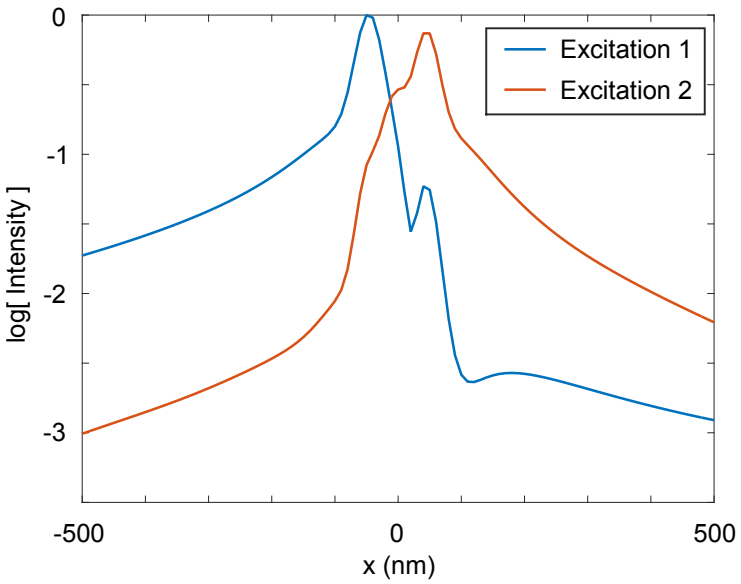

Fig. 6. The normalized intensity of the field radiated by the asymmetric dimer as a response to two different excitations. 1 - z-polarized excitation on the smaller MNP only, with $\omega =$ 4.50 rad/fs; 2 - both particles excited by an equal z-polarized electric field at both particles, with $\omega = 4.85$ rad/fs. The intensity is calculated along a line parallel to and at a height of 5 nm above the substrate, and with $y = 0$ nm.

this directionality is an inherent property: it is embedded in the normal modes. For the system under consideration, modes are found which can have an efficiency of SPP excitation in one direction which is more than two orders of magnitude higher than in the opposite direction. Although a complicated excitation setup is needed to exclusively excite the mode with the highest directionality, it is shown that even with a local or plane wave excitation an efficient directional response with a contrast of one order of magnitude can be achieved. The asymmetric dimer above a metallic substrate is the simplest class of systems in which this effect inherently embedded. It will be present for an asymmetric chain of MNPs, independently of the chain length. The contrast is expected to be higher for larger systems, because the radiation transverse to the chain direction can be canceled by destructive interference, as is known for phased array and Yagi-Uda antennas [30,31,33]. Since the proposed mechanism is based on the interference between the direct interaction of the MNPs and the interaction via the substrate, the system can be tuned and optimized by varying the inter-particle spacing, the distance to the substrate, the type of material, and the shape of the particles. In addition, this method can be straightforwardly extended to the directional excitation of the guided modes of dielectric waveguides. We envision the proposed mechanism to be a very useful tool in the design of directional couplers and antennas in layered media.

Acknowledgements

This work is supported by NanoNextNL, a micro and nanotechnology consortium of the Government of the Netherlands and 130 partners.

#255340 Received 8 Dec 2015; revised 20 Jan 2016; accepted 21 Jan 2016; published 16 Feb 2016

A. Non-orthogonal modes

In the presence of losses, the quasi-normal modes of the system will not be orthogonal in general. However, they do form a complete set and therefore, that they span the whole space. This implies that it is possible to write any dipole vector $\mathbf{p}$ as a superposition of the normal modes, i.e.

$$\mathbf{p} = a_1\mathbf{v}_1 + a_2\mathbf{v}_2, \tag{6}$$

where $\mathbf{v}_{1,2}$ are the normal modes, and $a_{1,2}$ the corresponding coefficients. In order to find the coefficients for the situation when $\mathbf{v}_1$ and $\mathbf{v}_2$ are not orthogonal, but are linearly independent, one can construct a so-called bi-orthogonal system. This is a related system consisting of the non-orthogonal vectors $\mathbf{v}^1$ and $\mathbf{v}^2$ with the property that $\mathbf{v}^i\mathbf{v}_j = \delta_{i,j}$, where $\delta_{i,j}$ is the Kronecker delta. Such a system can easily be found by taking the inverse of the matrix of which the columns are the normal modes. The row vectors of the inverse will form a set which is orthogonal to the normal modes. Therefore, the coefficients a_i can be easily found by calculating $\mathbf{v}^i\mathbf{p}$ and the dipole vector $\mathbf{p}$ can be written as a superposition of the normal modes of the system.

B. Calculation of the Sommerfeld integrals for complex frequencies

The interaction via the metallic substrate can be calculated using the method proposed by Sommerfeld. This procedure has been studied and described extensively in the literature. A very clear derivation of all the relevant equations can be found in, e.g. [58, 59]. The basic ingredient in the method is the so-called Sommerfeld identity,

$$\frac{e^{ik_1R}}{R} = i\int_0^\infty dk_\rho \frac{k_\rho}{k_{1,z}} J_0(k_\rho\rho)e^{ik_{1,z}|z|}, \quad k_{1,z} = \sqrt{k_1^2 - k_\rho^2}. \tag{7}$$

This states that one can write the spherical wave as a product of cylindrical waves in the ρ direction and plane waves in the z direction, summed over all in-plane wave numbers. In this equation R is the distance between the source and the point of measurement, $\rho = (x^2+y^2)^{1/2}$ the distance parallel to the substrate, k_1 the wavevector in the medium, and k_ρ and $k_{1,z}$ the wavevectors parallel and perpendicular to the substrate, respectively. Note that the effect of the substrate is not in the equation yet, it is only an expansion of the field in waves propagating parallel and perpendicular to the xy-plane.

Since only the plane waves will encounter the substrate, the influence of the substrate only has to be taken into account for those and has the well known form of the Fresnel reflection coefficients

$$r^s = \frac{\mu_2 k_{1,z} - \mu_1 k_{2,z}}{\mu_2 k_{1,z} + \mu_1 k_{2,z}}, \quad r^p = \frac{\varepsilon_2 k_{1,z} - \varepsilon_1 k_{2,z}}{\varepsilon_2 k_{1,z} + \varepsilon_1 k_{2,z}}, \quad k_{i,z} = \sqrt{k_i^2 - k_\rho^2}, \tag{8}$$

where ε_i and μ_i are the permittivity and permeability of medium i. Furthermore, k_i represents the wavevector in medium i and $k_{i,z}$ is the wavevector normal to the interface pointing into medium i. Now the Green's tensor for the interaction with the substrate can be constructed by splitting Eq. (7) for s and p polarization and multiplying it with the corresponding reflection coefficient [58]. As an example the zz-component of the tensor will be

$$\mathbf{G}_{zz}^{\text{ref}} = i\int_0^\infty \frac{k_\rho^3}{k_1^2 k_{1,z}} \left(\frac{\varepsilon_2 k_{1,z} - \varepsilon_1 k_{2,z}}{\varepsilon_2 k_{1,z} + \varepsilon_1 k_{2,z}}\right) e^{ik_{1,z}(z+h)} dk_\rho \tag{9}$$

Taking a close look at Eq. (9), one notices that there are two double-valued functions present, $k_{1,z}$ and $k_{2,z}$. In order to ensure convergence, it is important that the proper Riemann sheet is

#255340 Received 8 Dec 2015; revised 20 Jan 2016; accepted 21 Jan 2016; published 16 Feb 2016

selected, i.e. $\mathrm{Im}[k_{i,z}] > 0$. Both these functions give rise to a branch point at k_i and a corresponding branch cut. Furthermore, in the case of a metal substrate, the reflection coefficient r^p will have a singularity at $k_\rho = (\varepsilon_1\varepsilon_2/(\varepsilon_1+\varepsilon_2))^{1/2}$, the surface plasmon polariton.

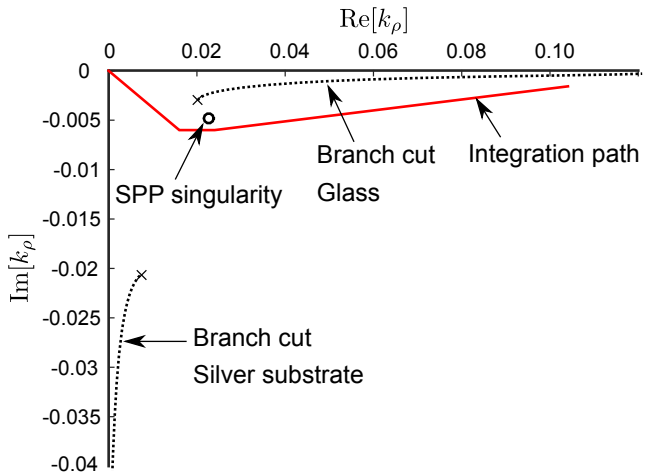

Fig. 7. A typical form of the integration path. The dotted lines represent the branch cuts corresponding to the glass medium and the silver substrate. The circle indicates the position of the singularity of r^p, i.e. the SPP. The frequency considered here is $\omega = 4 - 0.6i$.

A very fast and stable method to numerically evaluate these type of integrals was proposed by Paulus *et al.* [60]. For real frequencies, both the branch points and the singularity will lie in the first quadrant, and, being functions of ω, their exact position will depend on ω. Close to these points the integrand will have rapid oscillations which make the numerical evaluation complicated. The proposed method is to deform the integration path into the fourth quadrant, staying away from the difficulties. This yields a rapid and accurate calculation of the field.

However, for complex frequencies, as we are dealing with in this study, the singularity and the branch points will move into the fourth quadrant and in order to achieve convergence, the integration path also has to be in this quadrant. Furthermore, the Bessel function grows rapidly when the path is deformed too far away from the real axis. For accurate and fast evaluation, the integration path has to be chosen very carefully for each frequency in such a manner that the branch cuts and the singularity are avoided, while not moving too far away from the real axis.

An example of an integration path is shown in Fig. 7. The branch cuts arise from the double-valued functions $k_{i,z}$ for both media. The branch points corresponding to the glass medium, $\pm k_1$, are connected through $Re[k_\rho] \to \infty$, and $\pm k_2$, i.e. the branch points corresponding to the silver substrate, are connected through $Im[k_\rho] \to \infty$. The circle indicates the position of the singularity of r^p, which is corresponding to the surface plasmon polariton of the glass-silver interface.

#255340 Received 8 Dec 2015; revised 20 Jan 2016; accepted 21 Jan 2016; published 16 Feb 2016